

Design of tele-operated robot using UVC radiation for disinfection in surfaces Diseño de un robot tele-operado que utiliza radiación UVC para la desinfección de superficies

G. G. Sánchez-Hernández ^a, M. Hernández-Chávez ^a, J. D. Rivera-Fernández ^a,

K. Roa-Tort ^a, J. Gudiño-Sánchez ^a, D. A. Fabila-Bustos ^{a,*}

^aLaboratorio de Optomecatrónica y Energías, UPIIH, Instituto Politécnico Nacional, Distrito de Educación, Salud, Ciencia, Tecnología e Innovación, San Agustín Tlaxiaca, 42162, Hidalgo, México

Abstract

COVID-19 is the disease caused by a new strain of coronavirus known as SARS-CoV-2. The World Health Organization (WHO) first became aware of the existence of this new variant of the virus on December 31, 2019, and this disease was declared a pandemic on March 11, 2020, by the same organization. In this sense several tools for disinfection in air and surfaces have been proposed, considering not only this disease but also future outbreaks or pathologies with similar transmission patterns. By this reason, in this work we present the design and implementation of a UVC disinfection robot. The robot is composed of a mobile base with dimensions of 416 x 406 x 192 mm, which has four omnidirectional tires, and on each of the faces it has ultrasonic sensors for detecting obstacles. Also, on the front part of the base there is a camera that allows the user to view the route they take. On the other hand, the robot has a hexagonal-shaped support where six UVC radiation lamps with a maximum emission wavelength of 254 nm were placed. Likewise, the radiation pattern emitted was measured using a radiometer. After construction, performance tests were carried out to evaluate the appropriate dose for the elimination of bacteria. Measurements were carried out in classrooms by taking reference samples from the worktables that have plastic surfaces. It was determined that the appropriate dose for disinfection is 24.86 $\mu\text{W}/\text{cm}^2$, based on the results obtained in cultures carried out.

Keywords: Optomechatronics system, Disinfection, Ultraviolet radiation, COVID-19.

Resumen

La COVID-19 es la enfermedad causada por una nueva cepa de coronavirus conocida como SARS-CoV-2. La Organización Mundial de la Salud (OMS) tuvo conocimiento de la existencia de esta nueva variante del virus el 31 de diciembre de 2019, y declaró la enfermedad como pandemia el 11 de marzo de 2020. En este sentido, se han propuesto diversas herramientas para la desinfección del aire y de las superficies, considerando no solo esta enfermedad, sino también futuros brotes o patologías con patrones de transmisión similares. Por esta razón, en este trabajo se presenta el diseño e implementación de un robot de desinfección con radiación UVC. El robot está compuesto por una base móvil con dimensiones de 416 × 406 × 192 mm, que cuenta con cuatro ruedas omnidireccionales y sensores ultrasónicos en cada una de sus caras para la detección de obstáculos. En la parte frontal de la base se encuentra una cámara que permite al usuario visualizar la trayectoria del robot. Por otro lado, el robot posee un soporte de forma hexagonal donde se colocaron seis lámparas de radiación UVC con una longitud de onda máxima de emisión de 254 nm. Asimismo, se midió el patrón de radiación emitido mediante un radiómetro. Después de la construcción, se realizaron pruebas de rendimiento para evaluar la dosis adecuada para la eliminación de bacterias. Las mediciones se llevaron a cabo en aulas, tomando muestras de referencia de las mesas de trabajo con superficie plástica. Se determinó que la dosis apropiada para la desinfección es de 24.86 $\mu\text{W}/\text{cm}^2$, con base en los resultados obtenidos en los cultivos realizados.

Palabras Clave: Sistema optomecatrónico, Desinfección, Radiación ultravioleta, COVID-19

1. Introduction

Light is a form of electromagnetic energy that is often so ubiquitous in the daily lives of humans that its importance is

typically overlooked; however, it plays a crucial role in various biological and technological processes. Particularly, ultraviolet (UV) light has been employed for decades disinfection applications owing to its ability to deactivate pathogenic

*Autor para la correspondencia: dfabilab@ipn.mx

Correo electrónico: gsanchezh1502@alumno.ipn.mx (Germán Gerardo Sánchez Hernández), mhernandezch@ipn.mx (Macaria Hernández Chávez), jdriveraf@ipn.mx (Josué Daniel Rivera Fernández), kroat@ipn.mx (Karen Roa Tort), jgudinos@ipn.mx (Jesús Gudiño Sánchez), dfabilab@ipn.mx (Diego Adrián Fabila Bustos)

microorganisms (Darnell et al., 2004; Heilingloh et al., 2020). UV disinfection systems are used in a variety of applications, including:

- **Water Treatment:** UV light is used to disinfect drinking water and wastewater, eliminating pathogenic microorganisms without the use of chemical products (Song et al., 2016).
- **Surface Disinfection:** In hospitals and laboratories, UV light is used to disinfect surfaces and equipment, reducing the risk of contracting nosocomial infections (Guimera et al., 2017; Zotesso et al., 2016). In this context, the implementation of autonomous or tele-operated robots equipped with UV-C lamps further enhances safety by minimizing human exposure to potentially contaminated environments during the disinfection process.
- **Air Conditioning and HVAC:** HVAC (Heating, Ventilation, and Air Conditioning) systems can incorporate UV light to disinfect the air and prevent the spread of diseases (Cattai et al., 2023; DeGraw, 2021).

UV light within the wavelength range of 200 to 280 nm (known as UV-C) possesses germicidal properties. This UV-C radiation can alter the DNA and RNA of bacteria, viruses, and other microorganisms, preventing their replication and causing their inactivation. This process is particularly valuable in critical hygiene environments, such as hospitals, laboratories, schools, the food industry, among other places (Rudhart et al., 2022; Pereira et al., 2023).

Furthermore, the integration of optomechatronic technologies with UV disinfection systems has allowed for the development of more efficient and precise solutions (Soro et al., 2022). Optomechatronics is a discipline that combines optics, mechanics, electronics, and control to develop integrated systems with applications across various engineering and technological fields. These systems can include optical sensors, actuators, electronic control mechanisms, and signal processing, aimed at performing complex tasks with high precision and efficiency. This interdisciplinary integration leverages the strengths of multiple technological disciplines to achieve advanced functionality (Cho, 2005; Giesko & Mazurkiewicz, 2017).

The combination of optomechatronic technologies with UV disinfection systems has significantly improved their efficiency and control (Peñacoba et al., 2024). Some notable applications include:

- **UV Light Sensors:** These sensors measure the intensity of UV light and ensure that levels are sufficient for effective disinfection, automatically adjusting power as needed (Cullinan et al., 2023).
- **Automated Control Systems:** Automated systems control the duration and intensity of UV light exposure, optimizing the disinfection process and reducing energy consumption (Wang et al., 2022).
- **Disinfection Robots:** Robots equipped with UV-C lamps can autonomously navigate specific areas, providing uniform disinfection while avoiding direct human exposure to UV radiation (Pfleger et al., 2025; Fan et al., 2021).

In robotics, UVC disinfection has gained importance due to the COVID-19 pandemic. The company Geek+ developed the Lavender robot, capable of eliminating 99.99 % of pathogens with 253.5 nm UVC lamps, operating autonomously with

configurable disinfection modes (Geek+ Robotics, 2021). Meanwhile, Andersen et al. introduced a programmable robot that disinfects using dry aerosolized hydrogen peroxide for operating rooms and medical facilities.

These developments highlight the growing integration of robotics and optical disinfection to reduce human exposure and enhance sanitization efficiency. However, current systems are often costly or require complex infrastructure. This work therefore proposes a low-cost tele-operated UVC robot integrating CO₂ monitoring to support preventive disinfection in hospitals, schools, and public spaces.

Although the motivation initially arose during the COVID-19 pandemic, the system is not limited to SARS-CoV-2; UV-C light in the 200–280 nm range has been proven effective in inactivating a wide spectrum of microorganisms, including influenza viruses, coronaviruses, and various bacteria and fungi, by damaging their DNA and RNA structures.

The proposed design therefore contributes as a low-cost optomechatronic solution aimed at supporting preventive sanitary measures and environmental monitoring in medical, educational, and public facilities, strengthening disinfection protocols beyond pandemic-specific applications.

To validate the proposed design and assess its effectiveness, experimental tests were conducted in three main areas: (1) characterization of the UV-C lighting system, to determine the emission spectrum and irradiance of the lamps and confirm their germicidal effectiveness; (2) evaluation of the robot's mobility system; and (3) determination of the effective disinfection dose and exposure time, based on irradiance measurements obtained at different distances. These tests allowed validating the robot's capacity to safely and efficiently perform surface disinfection tasks.

2. Materials and methods

The development or design of a robot for UV-C light disinfection of surfaces and spaces such as laboratories, operating rooms, among others within hospitals, with CO₂ monitoring. It is noteworthy that a UV-C disinfection robot with air monitoring encompasses various primary functional areas to operate effectively and safely. These areas can be broadly defined as listed below:

- UV-C Lighting System or Source.
- Power Supply System.
- Robot Mobility System.
- Robot Physical or Structural System.
- Air Monitoring System.
- Control and Communication System.
- User Safety System.

To facilitate the description of the aforementioned functional areas, the robot shown in the Figure 1 plan will be used as a basis:

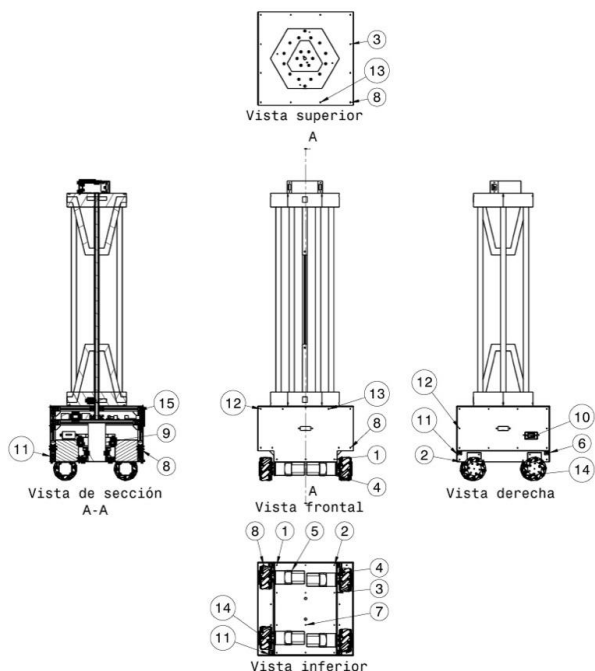


Figure 1: Visualization layout of a teleoperated mobile robot for UV-C light disinfection.

Figure 1 shows the design of a disinfectant robot with UV-C light from different perspectives and, Table 1 breaks down each of the indicated parts of the robot.

Table 1: Robot components description

Part number	Description
1	CO2 gas monitoring sensor and optical presence sensors to detect people in the area
2	Upper connection base for UV-C light lamps
3	Blacklight UV-C lamp
4	Lower connection base for UV-C light lamps
5	Upper acrylic plate of the robot base
6	Front ultrasonic sensor
7	Front acrylic plate of the robot base
8	Omnidirectional wheels
9	Stepper motors with reduction
10	Lower acrylic plate of robot base
11	Upper and lower lamp holders
12	Control circuitry and inverter (CD/CA converter)
13	Power batteries
14	Central support for lamps
15	Right side ultrasonic sensor
16	Power connection for battery charger
17	Right side acrylic plate of the robot base

When discussing a UV-C light disinfecting robot, a crucial component of the robotic device is undoubtedly the lighting system.

Ultraviolet light is generated both naturally and artificially. In its natural form, it comes from the sun; however, the atmosphere acts as a filter for most of this UV radiation. Therefore, artificial UV light generation is typically sought after for disinfection applications. Nowadays, LEDs and

fluorescent tube technologies are the most prominent. LEDs are more modern, offering advantages in durability and energy efficiency, but they are limited in the wavelengths they can achieve. On the other hand, fluorescent tubes, although older and less energy-efficient, remain widely used in germicidal applications because they can generate wavelengths around 254 nm, something that LED technology has not yet fully achieved. As a result, fluorescent tubes continue to be extensively utilized in germicidal applications (Memarzadeh et al., 2010).

Considering the wavelength of fluorescent tubes, they are very close to the peak of germicidal efficacy. The germicidal efficacy of UVC light peaks where it is most effective around 260–265 nm. This corresponds to the peak absorption wavelength of UV by bacterial DNA. For example, studies conducted with ultraviolet light and LED technology have determined that the most effective wavelength for inactivating the SARS-CoV-2 virus is 265 nm, achieving a 99% inactivation with a lower dose compared to other wavelengths such as 280 nm and 300 nm (Minamikawa et al., 2021).

Robot at Figure 1 uses fluorescent tube technology, marked with number 3. The optomechatronic disinfection device shown has six tubes. Considering that the robot was designed for SARS-CoV-2 virus disinfection, it was important to characterize the wavelength of the irradiation system. For this purpose, the QE65000AB spectrometer from Ocean Optics Corp. was used to obtain wavelength data emitted by the robot's lighting system, finding the peak emission at 254 nm and some components around 430 nm and 540 nm, as is shown in Figure 2.

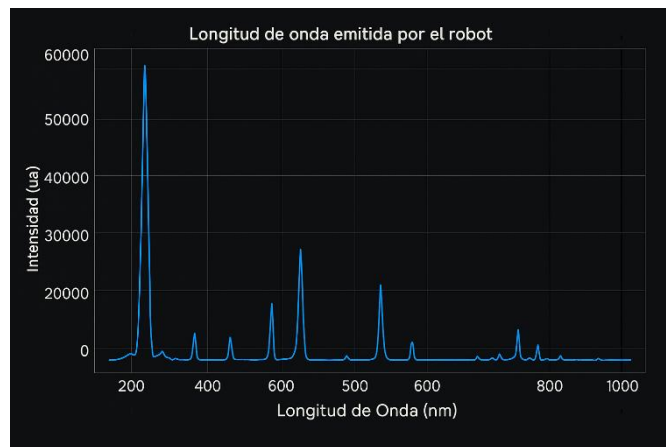


Figure 2: Emission spectrum of Blacklight UV-C lamp.

While the lighting system emits blue and red spectra, its main peak lies within the UV-C light range required for the application. Following the acquisition of the emission spectrum, it is necessary to determine its operation during the disinfection process; thus, calculating the disinfection time is required. In the specific case of the example robot, this was calculated at a distance of 80 cm from the position of the robot's lights. Once the distance is determined, the exposure time to UVC light is calculated. Initially, a theoretical value was determined based on the radiation value found in the lamp's datasheet, from which the system's irradiance was obtained using Equation 1.

$$I = \frac{P}{A} \quad (1)$$

Where:

I = irradiance [W/cm^2].

P = radiation power [W].

A = irradiation surface [cm^2].

Based on Equation 1, considering that each lamp has a power of 12 W and there are six lamps, theoretically yielding a total power of 72 W, and considering the distance of 80 cm from the ambient space, this theoretically means that the robot's effective area of action can be represented as the surface area of a sphere. Therefore, Equation 1 is expressed as follows.

$$I = \frac{72 \text{ [W]}}{4\pi \cdot (80^2) \text{ [cm}^2\text{]}} = 895.24 \text{ [}\mu\text{W/cm}^2\text{]} \quad (2)$$

Reported on [22], It mentions that the value of an adequate dose for the disinfection of the SARS- CoV-2 virus in spaces and surfaces is 10.6 mJ/cm^2 that's means $10600 \mu\text{W s/cm}^2$. With this value, it is possible to determine the required operating time of the robot for proper disinfection, such that the example robot can disinfect a space under the conditions described above in a time of 11.84 seconds. This was calculated using Equation 3.

$$t = \frac{\text{dosis}}{I} \quad (3)$$

Previously calculated value is a theoretical and ideal value, considering that the lamps radiate uniformly, but in reality, this is not usually the case. Therefore, it is necessary to measure the irradiance of each lamp and determine the real value by characterizing the system again. Consequently, tests were conducted to measure the radiant flux using the PM100D radiometer from Thorlabs Inc, to determine the irradiance at the required distance (80 cm). Figure 3 graphically shows the decay of the measured irradiance at different distances from the base of the robot.

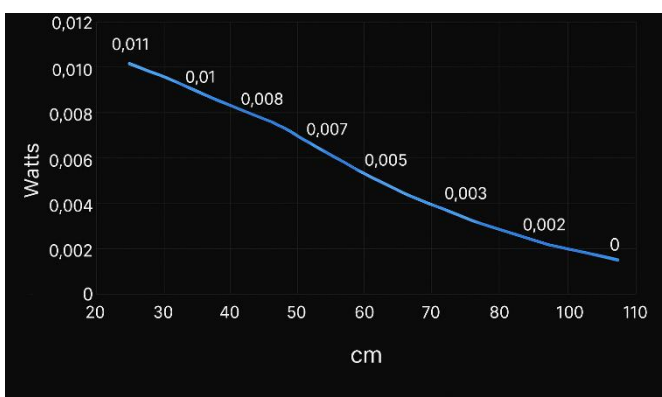


Figure 3: Decay of irradiance as a function of distance.

Making into account that the measurement at 80 cm is 0.002 W, the irradiance is recalculated using Equation 1, obtaining a value of $24.86 \mu\text{W}/\text{cm}^2$, which provides a total disinfection time in the estimated space of 7.1 minutes when considering the recommended dose in the study by Mankar et al. (2022) and the Equation 3.

As can be seen, it is crucial to consider that ideal values do not always directly correlate with the actual operational value of an optomechatronic system, such as radiation uniformity and power reported by the manufacturer and those obtained in tests at different distances.

2.1. Power Supply

Basically, all elements in the robot plan at Figure 1 that do not refer to a physical system component involve the robot's power and energy system. During the design of an optomechatronic UV-C disinfection system, it is important to consider the power consumption of each electrical and electronic component involved. However, this section will emphasize elements marked with numbers 12, 13, and 16 on the example robot plan. This focuses on the overall power system of the robot.

The disinfection system includes lithium batteries (element 13 on the plan) instead of lead-acid battery, thus two rechargeable LiFePO4 batteries were selected. These lithium-based batteries feature a lithium iron phosphate cathode and operate at 12.8 V with a nominal current capacity of 20 Ah. Two batteries are used: one powers only the UV-C lamps, and the other powers the motors, control board (Raspberry Pi 4), sensors, and a system monitoring camera. With these batteries, the robot can have an autonomy of 1 hour, considering that the lamps would be on all that time. This time would increase if the lamps were only turned on for controlled periods of time in an established routine.

In addition to the mentioned batteries, there is a 24 V to 5 A voltage regulator, also generally represented in item 12 of Figure 1. It is noteworthy that a 5 V power supply is required for general electronics operation, including sensors and the Raspberry Pi. Therefore, the robot includes the Xy-3606 voltage regulator module, chosen primarily because it meets the required voltage and current specifications.

On the other hand, it is important to note that this robot uses UV-C lamps powered by alternating current, so the system includes an inverter to convert direct current from the batteries to alternating current to power the lighting system. For this device, the main consideration was its ability to handle the power required by the six lamps, totaling 180 W. Therefore, the system incorporates the SP2-Q4000 converter from LSFYDYS, which has a power capacity of 4000 W, providing a safety margin just over two times the required power to account for any unforeseen circumstances, like a current surge and overheating. The general power supply scheme is illustrated in Figure 4. This picture shows the electronic implementation of the entire system includes the power batteries, the central control board Raspberry Pi 4, the voltage regulator, the DC/AC inverter, the lamps with their respective ballasts, ultrasonic sensors, CO₂ monitoring sensors, relays for stage coupling and power control, as well as the respective motor drivers with their corresponding stepper motor for robot mobility.

While the batteries serve as the power source for the described robot, a charger is required for them. Therefore, a connector was installed to recharge the system's power batteries, represented by number 16 at Figure 1, This is a generic connector for LiPo batteries.

In general, on Figure 4 the interconnection of each system and the importance of a power system for a mobile

disinfectant robot are evident. The following points will address details of each stage in the various systems that a disinfectant robot possesses analyzing the control and communication system, sensors for user safety, the physical structure, and, being a mobile robot, its mobility system.

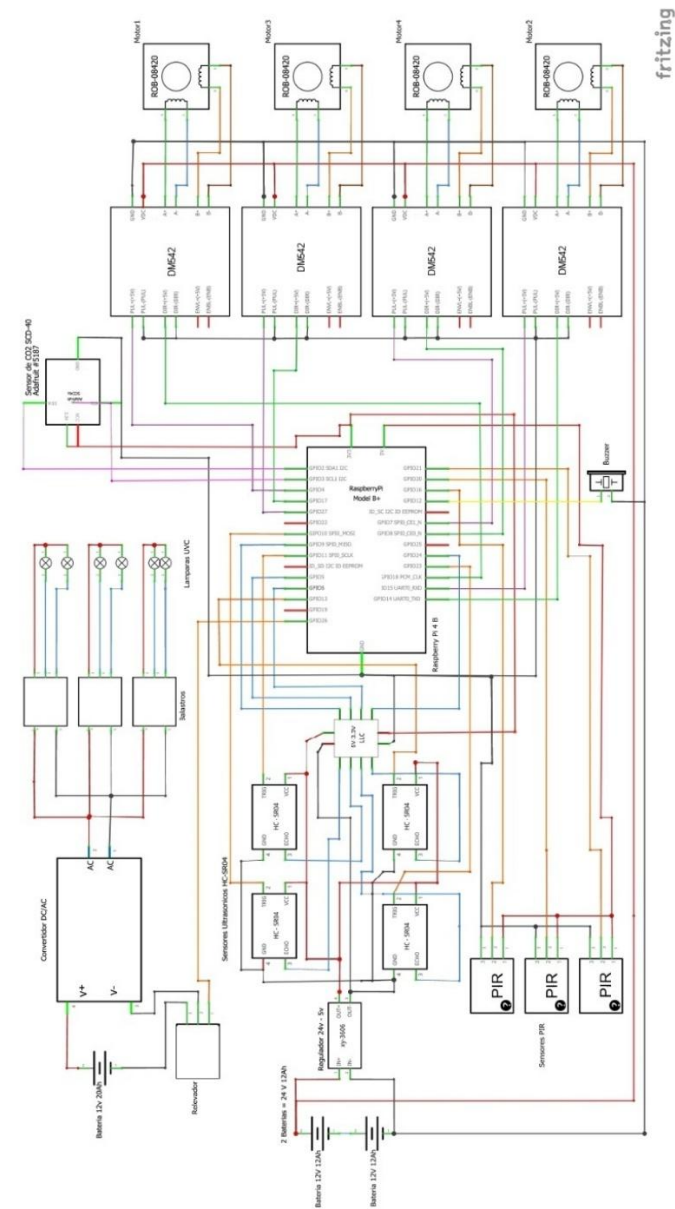


Figure 4: Electrical diagram of the robotic system

2.2. Robot Mobility System

Mobile robots have the capability to move autonomously or be teleoperated in both unknown and partially known environments (Bermudez, 2002). There are several ways to generate mobility in a robot. The methods and mechanisms used by the robot to move from one place to another are collectively known as locomotion. The mobility of a mobile robot depends directly on the terrain it operates on (Parsons, 2004).

In general, a mobile robot can have locomotion through wheels, tracks, hybrid systems, among others. For the described robot, the basic elements involved in the mobility

system are items numbered 8 and 9 (Figure 1) providing omnidirectional wheel locomotion to the robot.

Regarding the robot's wheels, item 8 on the robot plan, a mechanical omnidirectional system with four wheels is considered. It is important to note that the wheels must be arranged in a specific configuration due to their shape; incorrect placement can affect the robot's movement.

Figure 5 illustrates the arrangement that omnidirectional wheels must have based on the desired movement. Simply put, the proper arrangement of an omnidirectional wheel locomotion system should mimic the mechanical threads of a screw; otherwise, movements cannot be executed freely, hindering the robot's mobility.

The robot can move in any direction (forward, sideways, and rotation) thanks to its four omnidirectional wheels. The relationship between the wheel speeds ($\omega_1, \omega_2, \omega_3, \omega_4$) and the robot's motion (v_x, v_y, ω) can be described by simple equations. If the wheel radius is r and the distance from the center to each wheel is $(L + W)$, the wheel speeds are:

$$\begin{bmatrix} \omega_1 \\ \omega_2 \\ \omega_3 \end{bmatrix} = \frac{1}{r} \begin{bmatrix} 1 & -(L + W) \\ 1 & (L + W) \\ -1 & (L + W) \end{bmatrix} \begin{bmatrix} \omega_0 \\ \omega_0 \end{bmatrix} \quad (4)$$

These equations 4 allow the robot to move in any direction by adjusting the speed and direction of each motor.

Motors for generating the physical movement of the robot, there are distinct types, with the most popular for mobile robot implementation being DC motors and stepper motors when significant torque is required for mobility.

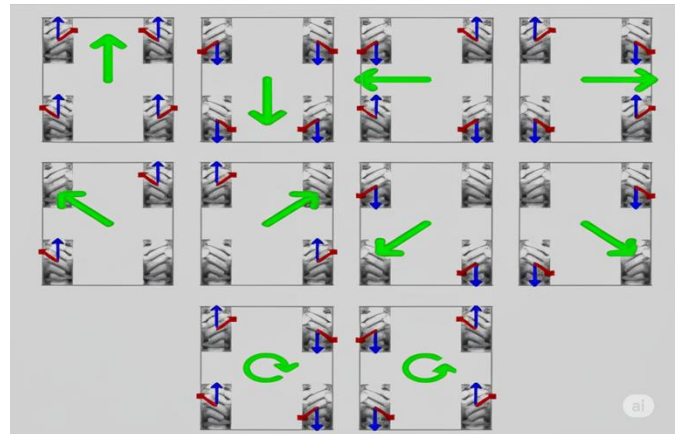


Figure 5: Arrangement of omnidirectional wheels for various movements.

It is important to consider that in the locomotion system, the power system plays a crucial role in energizing the motors. Additionally, another factor to consider is the total weight of the robot being moved. In the case of the disinfectant robot, item 9 consists of stepper motors with reduction gearing to increase torque and thereby support heavier loads.

As a first approach to determine the motor characteristics for designing the locomotion system of a mobile robot, it is important to consider the weight of all the elements that the system will support. Table 2 shows the weight of the total physical components of the robot.

Table 2: Weight of the physical components of the robot.

Component	Number of pieces	Weight (kg)
Motors	4	5.60
Batteries	3	3.66
Battery charger	1	0.35
Ballast	1	1.11
Blacklight UV-C lamp	6	0.81
DC/AC converter	1	1.36
Wheels	4	1.80
Chassis	-	6.00
Total		20.69

As shown in the preceding table, the total weight to be borne in order to move the robot is approximately 21 kg. Considering a 20% safety margin, it is estimated that a system capable of supporting up to 25 kg is needed. Considering that the wheels (item 8 in the robot's blueprint) have a diameter of 100 mm, factoring in both the maximum weight of the robot and the wheel diameter, the following outlines the process for calculating the required torque.

Firstly, a force diagram is considered to determine the elements influencing the operation of the robot. Figure 6 shows the force diagram considered for the robot in question. It is worth noting that while the robot will move in a "flat" environment, a safety factor for terrain irregularities considers a maximum inclination the robot can withstand of 10° .

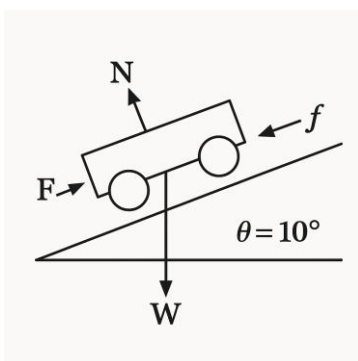


Figure 6. Force diagram for the mobile robot design.

From the previous diagram, the sum of forces along the x-axis is given by Equation 4.

$$\sum F_x = F - f - W \cdot \sin(\theta) = 0 \quad (5)$$

Where:

f = friction force of bearing [N]

F = minimum force required to break repose state [N]

W = robot weight [$kg \cdot m/s^2$]

T = inclination angle

From the previous elements, the value of f is calculated as indicated by Equation 5.

$$f = \frac{W \cdot \cos(\theta) \cdot a}{r} \quad (6)$$

Where:

a = rolling resistance coefficient [m]

r = wheels' radius [m]

W = robot weight [$kg \cdot m/s^2$]

θ = inclination angle

Considering solid rubber wheels implemented in this robot, with $a = 1.016$ mm, this gives $f = 4.9$ N when using Equation 5. Substituting this into Equation 4 yields $F = 47.49$. With this final value, the required torque for the motors can be calculated using Equation 6.

$$\tau = Fr \quad (7)$$

Where:

τ = torque [Nm]

F = minimum force required to break repose state [N]

r = wheels' radius [m]

Through equation 6, the motor requires a torque of 2.37 Nm. Considering that the robotic system has four wheels, each driven by a motor, the required torque for each motor would therefore be one-fourth of the calculated value, resulting in a required torque per motor of $0.5925 \text{ Nm} \approx 0.6 \text{ Nm}$, using a save factor of 2, the required torque will be 1.2 Nm.

Here was show how a locomotion system is determined using omnidirectional wheels and stepper motors with reduction for the design of a mobile disinfecting robot. Up to this point, it has addressed elements of the physical structure that influence the described systems. Therefore, the physical configuration of the robot also plays a crucial role.

3. Results and Discussion

The physical structure of the robot is an essential element when designing any robotic system, and it must be considered for the implementation of a UV light disinfection robotic device during its design phase. For the described robot, elements 5, 7, 10, and 17 (Figure 1) represent the 6 mm acrylic plates that cover the robot. Even in the case of the side plates, it should be noted that the diagram only shows the right-side plate, while the robot also has an identical plate on its left side that is not visible. The same applies to the front plate, as there is also a rear plate present. Although they are not explicitly shown in Figure 1. Each plate is supported using V-slot 2020

aluminum structural profiles, with appropriate hardware to provide robustness and stability to the robot, show Figure 7.

The same profile is used for the central support of the lamps (item 14 in the robot's reference plan).



Figure 7: Aluminum V-slot 2020 structural profiles and their mechanical assembly.

Similarly, there are machined parts and 3D-printed pieces for couplings and fastenings required to assemble the entire system. These pieces can be seen with numbers 2 and 4, specifically detailed in Figure 8 and the 11 y 14 are better appreciated on Figure 9.



Figure 8. Top and bottom mounting base for UV-C light lamps.



Figure 9. Upper lower and central holders' lamps.

Once all parts are assembled, the entire physical system is complete, which in terms of design can be seen from Figure 1. However, the final system, it is possible to visualize with more detail in Figure 10.

Up to this point, the described systems primarily cover the mechanical aspects of the robot (physical structure and locomotion system), the main UV-C irradiation system, and the central power system. However, another crucial aspect is the electronic system, encompassing sensors, communication, and robot control, including air quality monitoring.



Figure 10. Final view of the mobile robot.

3.1. Air Monitoring System

Monitoring environmental conditions in a disinfecting robot is crucial for its implementation, especially in the case of a robot designed to eradicate the SARS-CoV-2 virus. Monitoring CO₂ levels is particularly important in this context because carbon dioxide levels in indoor spaces can indicate air quality and ventilation effectiveness. Poor ventilation can increase the risk of virus transmission, as it primarily spreads through respiratory aerosols, which can accumulate in poorly ventilated indoor spaces (Bazant et al., 2021).

Monitoring CO₂ levels in the environment is crucial for disinfecting against the SARS-CoV-2 virus for three main reasons:

- Indicator of ventilation: High CO₂ levels suggest inadequate air renewal, which could allow the accumulation of particles capable of spreading the virus (Bazant et al., 2021).
- Reduction of transmission risk: Proper ventilation reduces the concentration of viral aerosols in the air, thereby lowering the likelihood of inhaling infectious particles (Morawska & Cao, 2020).
- Control in public spaces: In places like schools, offices, and public transportation, CO₂ monitoring can ensure safe air conditions (Burrige et al., 2021).

Therefore, the described robot is equipped with an air monitoring system using a CO₂ sensor, marked as numeral 1 in Figure 1, sensor used is the SCD-40, which have a

measurement range of 400 to 2000 ppm and accuracy of ± 40 ppm.

The sensor is configured to monitor every 5 seconds, detecting increases in ppm levels. Additionally, a sound buzzer has been connected to activate when the sensor reading exceeds 1000 ppm, remaining active until the value returns to a safe level. This serves as an indicator for individuals in enclosed environments to evacuate and allow the robot to initiate the disinfection process. This safety measure for users will be discussed further later on.

3.2. Control and Communication System

Robotic systems used in disinfection operations are typically autonomous or teleoperated. The robot described here is a teleoperated system that communicates via Wi-Fi protocol, allowing users to access and control the robot through a web application.

To remotely control the robot beyond the reach of UV-C light, a web application has been developed on a server using the Flask microframework, written in the Python programming language. This framework enables bidirectional communication between the control board and the controlling device, as depicted in Figure 11. By developing the application in Flask, any device connected to the same network can control the robot.

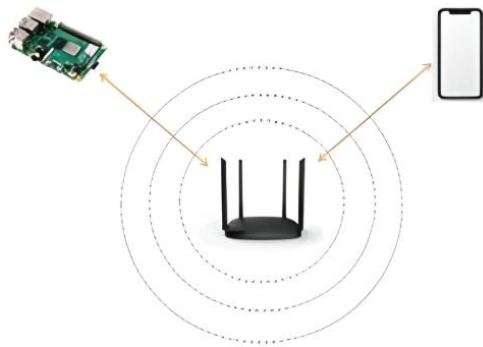


Figure 11. Bi-directional communication with a router.

The scheme depicted in Figure 11 shows the connection between the control board, a Raspberry Pi 4, and a mobile device via a router that establishes a Wi-Fi signal for bidirectional communication with the server. However, Wi-Fi internet connection is not always available everywhere. Therefore, a local network was set up using the Wi-Fi connectivity of the Raspberry Pi 4, achieved with Linux-compatible software called Host APD, designed to create Wi-Fi access points. With this setup, there is no longer a need to directly use a router to link the systems.

The discussion involves a mobile device controlling the robot through communication with a control board. For this purpose, a web application has been developed in Python, linked to various Flask routes, enabling execution upon accessing the network IP address hosting the server's web page. The operator's view of the robot is through a web page developed in HTML, CSS, and JavaScript.

This web page includes information from distance ultrasonic sensors, a CO₂ sensor, and live video transmission from a camera. These elements help guide the operator in manipulating the robot, providing controls for this action. All

necessary data and information are transmitted from the board to the server and to the client, which in this case is the device connected to the web page, as Figure 12 shown. The interface runs on a tablet.

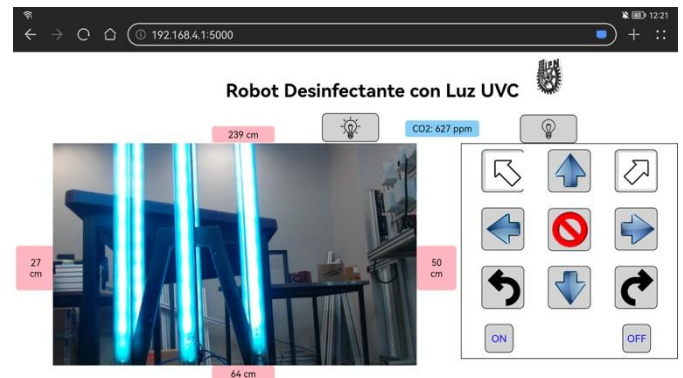


Figure 12. Web page for the graphical user interface (GUI) for control.

Generally, the robot's communication and control process follow the following algorithm, starting from powering on the robot when the area is clear of people, to executing the disinfection process. The startup involves connecting and synchronizing with the server via the aforementioned web application. Once the connection is established, data transmission from sensors (such as distance and CO₂ sensors) to the server begins, enabling the operator to monitor environmental conditions. Subsequently, controls are activated to initiate the disinfection process, which includes operating irradiation devices and other necessary components for the task. This workflow ensures the robot can operate safely and effectively in various environments.

1. **Power on:**
 - Start the system.
 - Proceed to the next step.
2. **Constant CO₂ sensor measurement:**
 - Continuously measure CO₂ levels in the environment using the sensor.
3. **Measurement greater than 1000ppm:**
 - Check if the CO₂ measurement exceeds 1000 ppm.
 - If greater than 1000 ppm, activate an alert (step 4).
 - If not, continue measuring (return to step 2).
4. **Alert activation:**
 - Activate an alert to indicate high CO₂ levels.
 - Proceed to step 5.
5. **Turn on motors:**
 - Turn on the robot's motors to start movement.
 - Proceed to step 6.
6. **Robot movement:**
 - The robot moves to perform the monitoring or disinfection task.
 - Proceed to step 7.
7. **Wi-Fi network execution and server execution:**
 - Activate the Wi-Fi

network and execute the server to allow remote communication and control.

- Proceed to step 8.
- 8. **Mobile connection:**
 - Check if a mobile connection is available.
 - If connected, transmit data (step 9).
 - If not, continue monitoring (return to step 7).
- 9. **Transmission of sensor, video, and control data:**
 - Transmit sensor, video, and control data over the network.
 - Proceed to step 10.
- 10. **Turn on UVC lights:**
 - Turn on the UVC lights to start disinfection.
 - Proceed to step 11.
- 11. **Presence detected:**
 - Check if presence is detected in the area.
 - If presence is detected, perform UVC irradiation (step 12).
 - If not, continue monitoring (return to step 10).
- 12. **UVC irradiation:**
 - Perform UVC irradiation to disinfect the area.
 - Proceed to step 13.
- 13. **Fulfill established irradiation time:**
 - Check if the established irradiation time has been fulfilled.
 - If fulfilled, proceed to final disinfection (step 14).
 - If not, continue irradiating (return to step 12).
- 14. **Disinfection:**
 - Complete the disinfection of the area.
 - End the process.

Generally, the control and communication system for a teleoperated mobile robot designed for UV-C disinfection in enclosed spaces has been presented as part of an optomechatronic system. However, one critical aspect of the design yet to be addressed is the safety of both users and the robot's operation. Implementing robust safety measures is essential to ensure the robot operates safely in dynamic and potentially hazardous environments, thereby protecting users and ensuring the effectiveness of disinfection operations.

3.3. User Safety System

In the design of a UV-C light disinfecting robot, user safety becomes a crucial priority. The radiation from this light spectrum poses significant risks to human health, including skin and eye damage, as well as effects on the immune system, due to its high energy and ability to interfere with DNA and RNA (Lindsley et al., 2015).

The robot presented in this chapter is equipped with multiple safety systems. Firstly, a CO₂ monitoring system with auditory alarm activation determines when individuals should

evacuate the area where the robot operates. Marked as numeral 1 on the robot's schematic diagram, it features infrared optical sensors to detect human presence, ensuring the robot automatically halts its functions when UV lights are active.

Additionally, the robot, capable of moving without activating its lights, incorporates ultrasonic sensors on all four sides. Numbers 6 and 15 on the robot's diagram (Figure 1) indicate the front and right-side sensors, replicated on the rear and left sides. These sensors only prevent collisions with obstacles, preemptively stopping the robot.

Figure 12 illustrates how these sensors continuously monitor the distance to nearby obstacles, updating readings every second.

Another notable component is a camera positioned at the robot's front, providing a remote view of the operational environment. This visual tool offers guidance to the operator, streaming real-time imagery of the surrounding area accessible via the user control web interface (see Figure 13 left side).

These safety elements are essential for a teleoperated robot in enclosed environments. It is important to note that mobile robots can adapt these systems or add others according to specific needs of their environment and application. In the case of the proposed design, it is possible to adapt to environments such as schools and hospitals, as its small size and the implemented systems make it safe for the environment and people.

3.4. Obtained Results

After the construction and testing of the proposed robot, several results were obtained regarding its functionality, efficiency, and safety performance. The robot exhibited stable control through the Wi-Fi interface, allowing smooth teleoperation and accurate command response. The UV-C disinfection system achieved an average irradiance of 24.86 $\mu\text{W}/\text{cm}^2$ at 80 cm, which is sufficient to inactivate different types of microorganisms. These results confirm that the emitted radiation and exposure time are adequate to ensure a proper germicidal effect on typical surfaces found in classrooms and laboratories. Among the main advantages of the system are its low cost, safe remote operation, modular structure, and stable omnidirectional mobility, which allows efficient maneuvering in confined environments. The hexagonal lamp arrangement provided uniform light distribution around the robot, minimizing shadowed zones and ensuring consistent UV exposure. The integration of a CO₂ monitoring system adds an additional safety layer, allowing users to evaluate air quality and ventilation during disinfection procedures.

Overall, the prototype successfully validated the feasibility of using a tele-operated optomechatronic platform for UV-C disinfection. Its architecture offers a practical and scalable solution that can be adapted for preventive sanitation in hospitals, schools, and public facilities. Future improvements will focus on extending battery life, integrating autonomous navigation with obstacle mapping, and implementing UV-LED arrays to enhance energy efficiency and reduce maintenance requirements.

4. Conclusions

In summary, the design of the mobile robot for disinfection using UV-C light represents a significant advancement in integrating optomechatronic technologies for sanitary applications. This device innovatively combines high-precision optical systems with robust mechanical systems, enabling efficient autonomous navigation and effective disinfection of enclosed spaces and surfaces without the disadvantages of manual and static UV methods. The use of UV-C light not only ensures effective elimination of pathogens but also reduces reliance on aggressive chemical methods, promoting safer and environmentally sustainable environments. With ongoing improvements in material durability, energy efficiency, and adaptability to diverse settings, this design could revolutionize disinfection practices in sectors such as healthcare, food industry, and beyond, positioning itself as a comprehensive and advanced solution for contemporary sanitary challenges.

References

- Bazant, M. Z., Kodio, O., Cohen, A. E., Khan, K., Gu, Z., & Bush, J. W. (2021). Monitoring carbon dioxide to quantify the risk of indoor airborne transmission of COVID-19. *Flow, 1*. <https://doi.org/10.1017/flo.2021.10>
- Bermudez, G. (2002). Robots móviles. Teoría, aplicaciones y experiencias. *Tecnura, 5*(10), 6-17. <https://doi.org/10.14483/22487638.5882>
- Burridge, H. C., Bhagat, R. K., Stettler, M. E. J., Kumar, P., De Mel, I., Demis, P., Hart, A., Johnson-Llambias, Y., King, M., Klymenko, O., McMillan, A., Morawiecki, P., Pennington, T., Short, M., Sykes, D., Trinh, P. H., Wilson, S. K., Wong, C., Wragg, H., . . . Linden, P. F. (2021). The ventilation of buildings and other mitigating measures for COVID-19: a focus on wintertime. *Proceedings Of The Royal Society A Mathematical Physical And Engineering Sciences, 477*(2247). <https://doi.org/10.1098/rspa.2020.0855>
- Cattai, F., D’Orazio, A., & Sbardella, G. (2023). A Systematic Review on the Application of Ultraviolet Germicidal Irradiation to HVAC Systems. *Energies, 16*(22), 7569. <https://doi.org/10.3390/en16227569>
- Cho, H. (2005). Optomechatronics. En *CRC Press eBooks*. <https://doi.org/10.1201/9781420039528>
- Cullinan, M. F., Scott, R., Linogao, J., Bradwell, H., Cooper, L., & McGinn, C. (2023). Development and Demonstration of a Wireless Ultraviolet Sensing Network for Dose Monitoring and Operator Safety in Room Disinfection Applications. *Sensors, 23*(5), 2493. <https://doi.org/10.3390/s23052493>
- Darnell, M. E., Subbarao, K., Feinstone, S. M., & Taylor, D. R. (2004). Inactivation of the coronavirus that induces severe acute respiratory syndrome, SARS-CoV. *Journal Of Virological Methods, 121*(1), 85-91. <https://doi.org/10.1016/j.jviromet.2004.06.006>
- DeGraw, J. (2021). *Ultraviolet Germicidal Irradiation for Heating, Ventilation, and Air Conditioning: Literature Review*. <https://doi.org/10.2172/1885363>
- Fan, Y., Hu, Y., Jiang, L., Liu, Q., Xiong, L., Pan, J., Hu, W., Cui, Y., Chen, T., & Zhang, Q. (2021). Intelligent disinfection robots assist medical institutions in controlling environmental surface disinfection. *Intelligent Medicine, 1*(1), 19-23. <https://doi.org/10.1016/j.imed.2021.05.004>
- Geek+ Robotics. (2021). Lavender: UV-C disinfection robot [Technical datasheet]. Geek Plus Technology Co., Ltd. <https://www.geekplus.com/products/lavender-uv-c-disinfection-robot>
- Giesko, T., & Mazurkiewicz, A. (2017). Applications of Optomechatronic Technologies in Innovative Industry. En *Lecture notes in mechanical engineering* (pp. 543-553). https://doi.org/10.1007/978-3-319-68619-6_52
- Guimera, D., Trzil, J., Joyner, J., & Hysmith, N. D. (2017). Effectiveness of a shielded ultraviolet C air disinfection system in an inpatient pharmacy of a tertiary care children’s hospital. *American Journal Of Infection Control, 46*(2), 223-225. <https://doi.org/10.1016/j.ajic.2017.07.026>
- Heilingloh, C. S., Aufderhorst, U. W., Schipper, L., Dittmer, U., Witzke, O., Yang, D., Zheng, X., Sutter, K., Trilling, M., Alt, M., Steinmann, E., & Krawczyk, A. (2020). Susceptibility of SARS-CoV-2 to UV irradiation. *American Journal Of Infection Control, 48*(10), 1273-1275. <https://doi.org/10.1016/j.ajic.2020.07.031>
- Lindsley, W. G., Martin, S. B., Thewlis, R. E., Sarkisian, K., Nwoko, J. O., Mead, K. R., & Noti, J. D. (2015). Effects of Ultraviolet Germicidal Irradiation (UVGI) on N95 Respirator Filtration Performance and Structural Integrity. *Journal Of Occupational And Environmental Hygiene, 12*(8), 509-517. <https://doi.org/10.1080/15459624.2015.1018518>
- Mankar, V., Dhengre, A., Agashe, N., Rodge, H., & Chandi, D. H. (2022). Ultraviolet irradiation doses for coronavirus inactivation -review and analysis of coronavirus photo inactivation studies. *International Journal Of Health Sciences, 466*-472. <https://doi.org/10.53730/ijhs.v6ns2.5038>
- Memarzadeh, F., Olmsted, R. N., & Bartley, J. M. (2010). Applications of ultraviolet germicidal irradiation disinfection in health care facilities: Effective adjunct, but not stand-alone technology. *American Journal Of Infection Control, 38*(5), S13-S24. <https://doi.org/10.1016/j.ajic.2010.04.208>
- Minamikawa, T., Koma, T., Suzuki, A., Mizuno, T., Nagamatsu, K., Arimochi, H., Tsuchiya, K., Matsuoka, K., Yasui, T., Yasutomo, K., & Nomaguchi, M. (2021). Quantitative evaluation of SARS-CoV-2 inactivation using a deep ultraviolet light-emitting diode. *Scientific Reports, 11*(1). <https://doi.org/10.1038/s41598-021-84592-0>
- Morawska, L., & Cao, J. (2020). Airborne transmission of SARS-CoV-2: The world should face the reality. *Environment International, 139*, 105730. <https://doi.org/10.1016/j.envint.2020.105730>
- Parsons, S. (2004). Introduction to Autonomous Mobile Robots by Roland Siegwart and Illah R. Nourbakhsh, MIT Press, 321 pp., \$50.00, ISBN 0-262-19502. *The Knowledge Engineering Review, 19*(4), 379-380. <https://doi.org/10.1017/s0269888905210354>
- Peñacoba, M., Bayona, E., Sierra-García, J. E., & Santos, M. (2024). Route Optimization for UVC Disinfection Robot Using Bio-Inspired Metaheuristic Techniques. *Biomimetics, 9*(12), 744. <https://doi.org/10.3390/biomimetics9120744>
- Pereira, A. R., Braga, D. F., Vassal, M., Gomes, I. B., & Simões, M. (2023). Ultraviolet C irradiation: A promising approach for the disinfection of public spaces? *The Science Of The Total Environment, 879*, 163007. <https://doi.org/10.1016/j.scitotenv.2023.163007>
- Pfleger, S. G., Haertel, M. E. M., & Della Mea Plentz, P. (2025). UV-C disinfection Robots: A Systematic review. *Journal Of Field Robotics*. <https://doi.org/10.1002/rob.22555>
- Rudhart, S. A., Günther, F., Dapper, L., Stuck, B. A., & Hoch, S. (2022). UV-C Light-Based Surface Disinfection: Analysis of Its Virucidal Efficacy Using a Bacteriophage Model. *International Journal Of Environmental Research And Public Health, 19*(6), 3246. <https://doi.org/10.3390/ijerph19063246>
- Song, K., Mohseni, M., & Taghipour, F. (2016). Application of ultraviolet light-emitting diodes (UV-LEDs) for water disinfection: A review. *Water Research, 94*, 341-349. <https://doi.org/10.1016/j.watres.2016.03.003>
- Soro, A. B., Shokri, S., Nicolau-Lapeña, I., Ekhlas, D., Burgess, C. M., Whyte, P., Bolton, D. J., Bourke, P., & Tiwari, B. K. (2022). Current challenges in the application of the UV-LED technology for food decontamination. *Trends In Food Science & Technology, 131*, 264-276. <https://doi.org/10.1016/j.tifs.2022.12.003>
- Wang, S., Li, Y., Ding, G., Li, C., Zhao, Q., Sun, B., & Song, Q. (2022). Design of UVC Surface Disinfection Robot with Coverage Path Planning Using Map-Based Approach At-The-Edge. *Robotics, 11*(6), 117. <https://doi.org/10.3390/robotics11060117>
- Zotosso, J. P., Cossich, E. S., Janeiro, V., & Tavares, C. R. G. (2016). Treatment of hospital laundry wastewater by UV/H2O2 process. *Environmental Science And Pollution Research, 24*(7), 6278-6287. <https://doi.org/10.1007/s11356-016-6860-5>